Speeding Up mmWave Beam Training through Low-Complexity Hybrid Transceivers

Joan Palacios*†, Danilo De Donno*, Domenico Giustiniano*, and Joerg Widmer*

*IMDEA Networks Institute, Madrid, Spain

Emails: name.surname@imdea.org

†Universidad Carlos III de Madrid, Spain

Abstract—Millimeter wave (mmWave) wireless technologies are expected to become key enablers of multi-gigabit wireless access in next-generation cellular and local area networks. Due to unfavorable radio propagation, mmWave systems will exploit large-scale MIMO and adaptive antenna arrays at both the transmitter and receiver to realize sufficient link margin. Unfortunately, power and cost requirements in mmWave radio front-ends make the use of fully-digital beamforming very challenging. In this paper, we focus on hybrid analog-digital beamforming and address two relevant aspects of the initial access procedure at mmWave frequencies. First, we propose a beam training protocol which effectively accelerates the link establishment by exploiting the ability of mobile users to simultaneously receive from multiple directions. Second, we deal with practical constraints of mmWave transceivers and propose a novel, geometric approach to synthesize multi-beamwidth beam patterns that can be leveraged for simultaneous multi-direction scanning. Simulation results show that the proposed hybrid codebooks are able to shape beam patterns very close to those attained by a fully-digital beamforming architecture, yet require lower complexity hardware compared with the state of the art. Furthermore, the reduced duration of the beam training phase, in turn enabled by the multi-beam characteristics of our hybrid codebooks, provides a 25% to 70% increase in spectral efficiency compared to existing sequential scanning strategies.

I. INTRODUCTION

Due to the spectrum fragmentation below 6 GHz, current wireless communication systems cannot support user data rates of several Gbps and above in a commercially viable manner. Such bandwidth shortage has motivated the exploration of vacant, unlicensed spectrum at higher frequencies, and in particular in the millimeter-wave (mmWave) frequency bands which the future fifth-generation (5G) wireless standard is expected to exploit [1], [2].

The higher propagation loss and unfavorable atmospheric absorption make data transmission over relatively long distances a serious challenge at mmWaves. The short wavelength, however, allows more antenna elements to be integrated into mmWave devices and enables large-scale multiple-input multiple-output (MIMO) and adaptive antenna arrays to overcome range limitations. Traditional MIMO processing as performed in sub-6 GHz systems is, at present, impractical at mmWaves because the high cost, power consumption, and complexity of mixed-signal hardware at such frequencies prevent the use of a dedicated RF chain per antenna element [3].

For this reason, most of the literature proposes analog/RF beamforming architectures which rely on networks of RF phase shifters to control the phase of the signal at each antenna element [4]–[7]. However, compared to fully-digital beam-forming architectures which can precisely control both phase and amplitude of the transmitted/received signals, analog beamforming is sub-optimal because of the constant amplitude and the low phase resolution constraints affecting the RF phase shifters currently available for mmWave frequencies [8]. Such constraints seriously impact the beamforming performance, resulting in antenna radiation patterns with (i) high, difficult-to-control sidelobe levels (SLLs), (ii) array gain dependent on the steering direction, and (iii) fixed beamwidth [9]. This latter point is crucial for the design of low-overhead, multi-level beam training protocols where the angular sector covered by the beam is wider in the earlier training stages and is progressively narrowed to a converging antenna pattern for subsequent data transmissions [4], [5]. Furthermore, since the transceiver can only use one beam direction at a time, analog beamforming lacks multi-direction searching, thus resulting in more time required for beam training. This leads to the well-known tradeoff between the time devoted to beam training (overhead) and the effective data rate [10], [11]. That is, increasing the alignment overhead leaves less time for data transmission, thus resulting in reduced transmission rates.

Hybrid analog-digital architectures aim at approaching the performance of fully-digital beamforming by dividing the pre-coding/combining operations between the analog and digital domains and adopting fewer RF chains compared to pure digital architectures. The availability of multiple RF chains allows hybrid analog-digital architectures to shape beam patterns very close to those attained by a fully-digital architecture, i.e., with limited overlap between adjacent beams and excellent flatness over the covered sectors. Moreover, since multiple RF chains used simultaneously provide multi-direction scanning, hybrid analog-digital architectures are able to speed up the beam training phase, hence increasing the effective data rate.

Despite the substantial research interest recently gained by hybrid beamforming for mmWave systems, to the authors' knowledge, only very few works in the literature have investigated the opportunity of leveraging the multi-direction scanning capabilities of hybrid transceivers to accelerate the beam training. For example, the acceleration of the cell discovery procedure is analyzed in [12] and the gain provided by hybrid beamforming is simply deduced based on the performance achieved for analog and digital beamforming. In

[13], the simultaneous, multi-direction scanning capabilities of hybrid transceivers are exploited to estimate the mmWave channel. The synthesis of hybrid analog-digital precoders and combiners is accomplished by a genetic algorithm whose notable complexity, however, hinders its implementation in resource constrained mobile devices.

Most of the literature on mmWave hybrid beamforming has, until now, considered sequential, single-direction scanning during the beam training phase, focusing the attention, instead, on the design of optimal precoders to achieve larger multiplexing gains during the data trasmission phase. However, the proposed solutions exhibit high computational complexity and rely on unrealistic hardware assumptions based on the availability of a considerable number of RF chains and RF phase shifters with large (or even infinite) number of quantization bits. In [14], a codebook design algorithm is developed under the assumption that hybrid analog-digital beamforming is used only at the transmitter while the receiver is equipped with a single antenna. The hybrid codebook is designed by minimizing the mean square error (MSE) between the code vector's beam pattern and its corresponding ideal beam pattern. The approximation of MSE minimization is accomplished by the orthogonal matching pursuit (OMP) algorithm with unconstrained digitally-controlled RF phase shifters (i.e., with infinite number of quantization bits). A similar OMP-based approach with unconstrained RF phase shifters is discussed also in [15]. A hybrid analog-digital codebook relying on beamforming vectors with different beamwidths and gains is presented, for the first time, in [16]. The ability to generate beams with various beamwidths makes such codebook particularly attractive for the design of adaptive, low-overhead beam training protocols. The approach in [16] assumes that RF phase shifters with a large number of quantization bits are available at mmWave frequencies. However, the current state of silicon technologies makes the design of RF phase shifters with high phase shift resolution challenging and even impractical [8].

In this paper, taking the work of [16] and [17] as a starting point, we propose and implement an adaptive, low-overhead beam training protocol exploiting the simultaneous, multi-direction scanning capabilities of hybrid analog-digital transceivers. To this end, we take into account practical constraints of mmWave transceivers and design a hybrid codebook to match the multi-beamwidth, multi-beam requirements of the proposed protocol. The contributions of this paper are as follows:

- We propose to speed-up the beam training process in mmWave systems by exploiting the simultaneous, multi-direction reception capability of hybrid analog-digital transceivers. To this end, we design an adaptive, low-overhead beam training protocol which incorporates such a capability;
- We formulate an optimization problem to approximate a fully-digital, multi-beam codebook by means of a hybrid architecture requiring a number of RF chains much lower than the number of antenna elements and only 2-bit RF phase shifters;

- We propose and implement a novel approach, based on geometric considerations, to efficiently solve the above optimization problem with much lower computational complexity and higher accuracy than OMP-based strategies in the literature. Our design enables simultaneous, multi-direction scanning and, therefore, can be leveraged in the framework of beam training to accelerate the mmWave link establishment.

Our solution is able to synthesize beam patterns almost indistinguishable from those shaped by fully-digital beamforming, although requires lower complexity hardware compared with the literature. Additionally, the speed up achieved by our beam training protocol determines a considerable rate increase compared to state-of-the-art strategies based on sequential, single-direction scanning during beam training.

II. SYSTEM MODEL

We consider the mmWave system shown in Fig. 1 and focus on the beam training phase during which a base station (BS) equipped with a uniform linear array (ULA) of M_{BS} isotropic radiators and $N_{\text{RF-BS}}$ RF transceiver chains uses a single stream of data to transmit training packets along one direction at each time slot. On the other side, a mobile station (MS) equipped with a ULA of M_{MS} isotropic radiators and $N_{\text{RF-MS}}$ RF transceiver chains performs signal-to-noise ratio (SNR) measurements simultaneously over multiple directions to speed-up the process. More concretely, the BS applies an $N_{\text{RF-BS}} \times 1$ digital baseband precoder $\mathbf{p}_{\text{BB}}$ followed by an $M_{\text{BS}} \times N_{\text{RF-BS}}$ RF precoder, $\mathbf{P}_{\text{RF}}$, to the discrete-time transmitted symbol $s(t)$ — the transmit power constraint is ensured by imposing the normalization $\|\mathbf{P}_{\text{RF}}\mathbf{p}_{\text{BB}}\|_2^2 = 1$. On the other side, the MS configures its front end to concurrently receive over $D \leq N_{\text{RF-MS}}$ different directions. To do that, it applies an $M_{\text{MS}} \times N_{\text{RF-MS}}$ RF combiner $\mathbf{C}_{\text{RF}}$ followed by a $N_{\text{RF-MS}} \times D$ digital baseband combiner $\mathbf{C}_{\text{BB}}$. The discrete-time signal received by the MS is the $D \times 1$ vector $\mathbf{y}(t)$ given by:

$$\mathbf{y}(t) = \sqrt{\rho}\mathbf{C}^H\mathbf{H}\mathbf{p}s(t) + \mathbf{C}^H\mathbf{n}(t) \tag{1}$$

where $\mathbf{C} = \mathbf{C}_{\text{RF}}\mathbf{C}_{\text{BB}}$ (dimensions $M_{\text{MS}} \times D$), $\mathbf{p} = \mathbf{P}_{\text{RF}}\mathbf{p}_{\text{BB}}$ (dimensions $M_{\text{BS}} \times 1$), ρ is the average received power, $\mathbf{H}$ is the $M_{\text{MS}} \times M_{\text{BS}}$ mmWave channel matrix, and $\mathbf{n}(t) \sim \mathcal{CN}(\mathbf{0}, \sigma^2\mathbf{I})$ is the complex white Gaussian noise.

Similarly to [14]–[16], we consider a narrowband block-fading propagation channel model which captures the geometrical structure and sparse nature of mmWave channels [18]:

$$\mathbf{H} = \sqrt{\frac{M_{\text{BS}}M_{\text{MS}}}{L}} \sum_{l=1}^{L} \alpha_l\mathbf{a}_{\text{MS}}(\psi_{\text{MS},l})\mathbf{a}_{\text{BS}}^H(\psi_{\text{BS},l}) \tag{2}$$

where L is the number of paths, $\alpha_l \sim \mathcal{CN}(0, 1)$ is the complex gain of the lth path, and $\mathbf{a}_{\text{MS(BS)}}(\psi_{\text{MS(BS)},l})$ is the ULA response vector at the MS (BS) whose expression can be found in [17, Eq. (3)]. Note that, in order to simplify the notation, we consider BS and MS implementing horizontal (2-D) beamforming only, which implies that all scattering happens in the azimuthal domain. Extensions to planar antenna
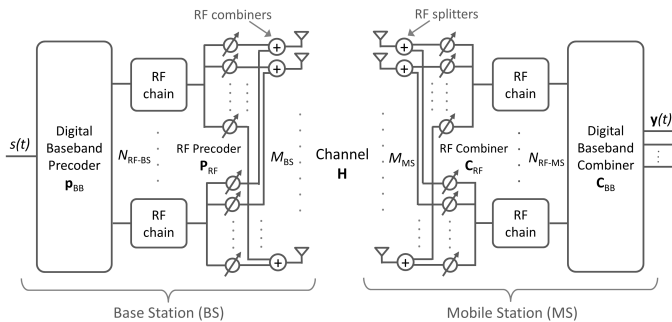
Fig. 1. Overview of the BS-MS mmWave transceiver architecture for hybrid analog-digital beamforming.
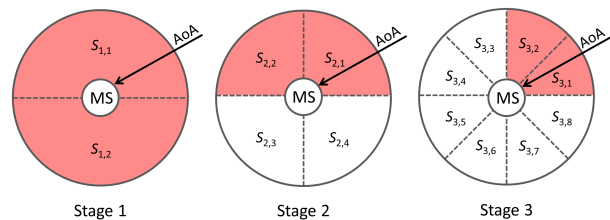

Fig. 2. An example of azimuthal domain partitioning performed by the MS during the adaptive beam training protocol for AoA estimation ($K=D=2$). The highlighted sectors are the ones covered simultaneously by the MS at each stage.

arrays and, therefore, to 3-D beamforming is straightforward as reported in [19].

Our objective is to *design a multi-beam, multi-beamwidth codebook based on the mmWave hybrid architecture in Fig. 1 and assuming RF phase shifters with few quantization bits*. In the next section, we illustrate how the simultaneous, multi-direction scanning capabilities enabled by such a codebook can be leveraged to design low-overhead beam training protocols for fast and adaptive angle of departure (AoD) and angle of arrival (AoA) estimation.

III. BEAM TRAINING PROTOCOL

We consider the beam training protocol used in our prior work [17], and first proposed in [16], where the beamforming vectors are adaptively configured at both the BS and MS sides based on the bisection concept. Starting from this basic algorithm, we design in this section a new beam training protocol accommodating MSs able to receive simultaneously from multiple directions as modeled in §II. Although the algorithm assumes the availability of a feedback channel between the BS and MS, such requirement can be easily relaxed by using the ping-pong approach described in [20].

At the beginning of the algorithm, the BS divides its $[0, 2\pi]$ azimuthal domain into K sectors, namely $S_{1,k}$ with $k = 1, 2, ..., K$, and designs the best hybrid analog-digital precoders **p** to transmit the beacon signal over such sectors at K successive time slots. At the same time, the MS also divides its azimuthal domain into K sectors, but it employs $\lceil K/D \rceil$ measurement matrices **C** at $\lceil K/D \rceil$ successive instants to detect, in parallel from D directions at each time slot, the beacon signal transmitted by the BS. In fact, the availability of multiple RF chains allows the MS to simultaneously "listen" to $D \leq N_{\text{RF-MS}}$ directions simultaneously[1]. The MS compares the SNR of the received beacon signals to determine the one with the maximum SNR. This translates into selecting the partition which is highly likely to contain the most dominant AoD/AoA of the mmWave channel. The MS then communicates the search results to the BS to prepare for the later stages

where the selected partition is further divided into smaller subsets until the AoD/AoA pair is estimated with the desired resolution. It is evident that increasing D likewise reduces the number of RF chains assigned to each scanned direction, which definitely affects the quality of the beam patterns. Such a qualitative evidence will be quantitatively evaluated later in §V.

An example of partitioning of the azimuthal domain performed by the MS during the first three stages of the beam training protocol with $K=D=2$ is reported in Fig. 2. In the first stage, the MS receives simultaneously from sector $S_{1,1}$ and sector $S_{1,2}$ and selects the former as the one with highest SNR. In the second stage, the sector selected in the previous stage ($S_{1,1}$) is further divided into two 90° sectors ($S_{2,1}$ and $S_{2,2}$) which are used simultaneously by the MS to perform SNR measurements. The process is repeated in the succeeding stages until the required angular resolution of the AoA estimation is achieved.

In case of reciprocal channel and time-slot duration T_{slot}, since K beamforming vectors are sequentially used at the BS and, for each of them, $\lceil K/D \rceil$ measurement vectors are sequentially employed at the MS, the total time required to estimate the most dominant AoD/AoA of the channel with angular resolution $2\pi/N$ becomes:

$$\tau = T_{\text{slot}} K \left\lceil \frac{K}{D} \right\rceil \log_K N \qquad (3)$$

This represents a significant speed up compared to the basic adaptive beam training protocol considered in [16] and [17] where the sequential reception at the MS produces an estimation time, τ_{seq}, which is D times higher than that calculated in Eq. 3:

$$\tau_{\text{seq}} = T_{\text{slot}} K^2 \log_K N \qquad (4)$$

In case of non-reciprocal channel, the beam training algorithm is repeated with **H** replaced by the uplink channel and the roles of the BS and MS reversed.

The AoD/AoA estimation accuracy achieved at the end of beam training critically depends on how well the adopted beam patterns approximate the ideal sectors in Fig. 2. In the next section, we present an algorithmic strategy to accurately approach fully-digital sector beams by means of a hybrid analog-digital architecture requiring very low complexity hardware.

[1]In principle, simultaneous, multi-direction transmission could be also exploited at the BS to further speed up the beam training, but this is left as future work.

IV. HYBRID ANALOG-DIGITAL BEAM PATTERNS

The problem of designing the best hybrid analog-digital precoder/combiner at the BS and MS sides can be translated into the one of designing, at each stage of the beam training protocol in the previous section, beam patterns with three main characteristics: (1) limited overlap with adjacent beams; (2) flat-top shape over the covered angular region; (3) limited number and intensity of side lobes.

In this section, we present a practical codebook design which relies on the availability of a hybrid analog-digital architecture with number of RF chains much lower than the number of antenna elements, and RF phase shifters with just four phase values $(0, \pm\pi/2, \pi)$ without amplitude adjustment.

We consider a mmWave system where the BS transmits a single stream of beam training data, i.e., it employs beam patterns covering only one of the white sectors in Fig. 2 at a time. On the other side, the MS adopts beam patterns able to simultaneously cover multiple sectors (for example, the red sectors in Fig. 2). We first discuss on the codebook design at the MS side. The introduced concepts can then be used to easily derive the codebook at the BS side as well.

At each stage of the adaptive beam training protocol illustrated in §III, the set of concurrent beam patterns — in the sequel also referred to as measurement vectors or combining vectors — used by the MS to receive beam training data can be arranged into a $M_{\text{MS}} \times D$ matrix $\mathbf{C} = \mathbf{C}_{\text{RF}}\mathbf{C}_{\text{BB}}$, where $D \leq N_{\text{RF-MS}}$ is the number of sectors which the MS is able to cover simultaneously, $\mathbf{C}_{\text{RF}}$ is the RF combining matrix, and $\mathbf{C}_{\text{BB}}$ is the digital baseband combining matrix. The problem of designing a hybrid analog-digital codebook with multiple simultaneous receive beams can be modeled by finding an RF (baseband) combiner $\mathbf{C}_{\text{RF}}^{\text{opt}}$ ($\mathbf{C}_{\text{BB}}^{\text{opt}}$) such that:

$$
\mathbf{C}_{\text{RF}}^{\text{opt}} = \arg\min_{\mathbf{C}_{\text{RF}}} \left\| \mathbf{C}_{\text{bsl}} - \mathbf{C}_{\text{RF}}\hat{\mathbf{C}}_{\text{BB}} \right\|_2
$$
$$
\text{s.t. } [\mathbf{C}_{\text{RF}}]_{:,i} \in \mathcal{C}_{\text{RF}}, \ i = 1, 2, ..., N_{\text{RF-MS}}
$$
$$
\hat{\mathbf{C}}_{\text{BB}} = \left(\mathbf{C}_{\text{RF}}^H \mathbf{C}_{\text{RF}} \right)^{-1} \mathbf{C}_{\text{RF}}^H \mathbf{C}_{\text{bsl}} \qquad (5)
$$
$$
\left[\mathbf{C}_{\text{BB}}^{\text{opt}} \right]_{:,i} = \frac{[\hat{\mathbf{C}}_{\text{BB}}]_{:,i}}{\| \mathbf{C}_{\text{RF}}[\hat{\mathbf{C}}_{\text{BB}}]_{:,i} \|_2}, \ i = 1, 2, ..., N_{\text{RF-MS}}
$$

where $\mathbf{C}_{\text{bsl}}$ is the matrix that contains the baseline array vector weights that are to be approximated. In this paper, we refer to baseline beam patterns as the beam patterns that can be synthesized by exploiting a fully-digital beamforming architecture where the availability of a dedicated RF chain for each antenna element enables precise control of both phase and amplitude of the mmWave signals. As in [17], we choose the sector beam design based on the Fourier Series Method with Kaiser windowing (FSM-KW) to synthesize beam patterns confined to a desired angular region [21, Chapter 21, pp. 946-949]. Compared to other windows such as Hamming, Blackman, etc., the Kaiser window has more design flexibility since the trade-off between the main lobe width and the sidelobe ripple amplitude can be accurately set by adjusting some window parameters.

Algorithm 1 A geometric approach to design hybrid analog-digital multi-directional beam patterns

Require: $\mathbf{C}_{\text{bsl}}$
1: $\mathbf{C}_{\text{RF}} = $ Empty matrix
2: $\mathbf{C}_{\text{res}} = \mathbf{C}_{\text{bsl}}$
3: **for** $n \leq N_{\text{RF-MS}}$ **do**
4:   $k = \arg\max_k \| [\mathbf{C}_{\text{res}}]_{:,k} \|_2^2$
5:   $\mathbf{c}_{\text{res}} = [\mathbf{C}_{\text{res}}]_{:,k}$
6:   $\mathbf{C}_{\text{RF}} = [\mathbf{C}_{\text{RF}}, \mathcal{S}(\mathbf{c}_{\text{res}})]$
7:   $\mathcal{M} = \max_i |\mathbf{c}_{\text{res}}(i)|, \ m = \min_i |\mathbf{c}_{\text{res}}(i)|$
8:   $J = \text{find} \left[|(\mathbf{c}_{\text{res}}| \geq \frac{\mathcal{M}+m}{2} \right]$
9:   $\delta' = \text{mean} \left[\mathbf{c}_{\text{res}}(J)/\mathcal{S}(\mathbf{c}_{\text{res}})(J) \right]$
10:   **if** $|\delta'| > \frac{\mathcal{M}+m}{2}$ **then**
11:    $\delta = \frac{\delta'}{|\delta'|}\frac{\mathcal{M}+m}{2}$
12:   **else**
13:    $\delta = \delta'$
14:   **end if**
15:   $\mathbf{c}_{\text{res}} = \mathbf{c}_{\text{res}} - \delta \mathcal{S}(\mathbf{c}_{\text{res}})$
16:   $[\mathbf{C}_{\text{res}}]_{:,k} = \mathbf{c}_{\text{res}}$
17:   **for** $i \leq D, \ i \neq k$ **do**
18:    $[\mathbf{C}_{\text{res}}]_{:,i} = [\mathbf{C}_{\text{res}}]_{:,i} - \mathcal{S}(\mathbf{c}_{\text{res}})\frac{[\mathcal{S}(\mathbf{c}_{\text{res}})]^H [\mathbf{C}_{\text{res}}]_{:,i}}{\| \mathcal{S}(\mathbf{c}_{\text{res}}) \|_2^2}$
19:   **end for**
20: **end for**
21: $\hat{\mathbf{C}}_{\text{BB}} = \left(\mathbf{C}_{\text{RF}}^H \mathbf{C}_{\text{RF}} \right)^{-1} \mathbf{C}_{\text{RF}}^H \mathbf{C}_{\text{bsl}}$
22: **for** $i \leq D$ **do**
23:   $[\mathbf{C}_{\text{BB}}]_{:,i} = \frac{[\hat{\mathbf{C}}_{\text{BB}}]_{:,i}}{\| \mathbf{C}_{\text{RF}}[\hat{\mathbf{C}}_{\text{BB}}]_{:,i} \|_2}$
24: **end for**
25: **return** $\mathbf{C}_{\text{RF}}, \mathbf{C}_{\text{BB}}$

The finite set of possible analog beamforming vectors is encompassed by the set $\mathcal{C}_{\text{RF}} \in \mathbb{C}^{M_{\text{MS}}}$ of vectors with components $\{\pm1, \pm j\}$, which is also referred to as dictionary in the sequel. Such constraint on $\mathbf{C}_{\text{RF}}$ translates into the hardware constraint of using RF phase shifters with just two quantization bits[2].

The problem stated in Eq. 5 can be solved using the OMP algorithm and its variants as proposed in most of the literature on hybrid analog-digital beamforming [14]–[17], [19]. Despite their simplicity and ease of implementation, OMP-based approaches share the disadvantage of high computational complexity — $O(N_{\text{RF-XX}}^4)$ due to a matrix inversion at each step — and reduced accuracy since they rely on non-complete dictionaries made of basis subsets. On the contrary, we propose a novel approach, based on geometric considerations and manipulations, to solve the problem in Eq. 5 with lower computational complexity — in the order of $O(N_{\text{RF-XX}}^3)$ — than OMP-based strategies. It is worth noting that, in contrast to the above mentioned literature which focuses on the design of hybrid codebooks covering only one sector at a time, our design enables the MS to simultaneously cover more than one sector during the beam training process. This translates into the problem of finding an optimal RF combiner $\mathbf{C}_{\text{RF}}$ for all

---

[2]The algorithm requires only minor modifications to accommodate RF phase shifters with a different number of quantization bits.
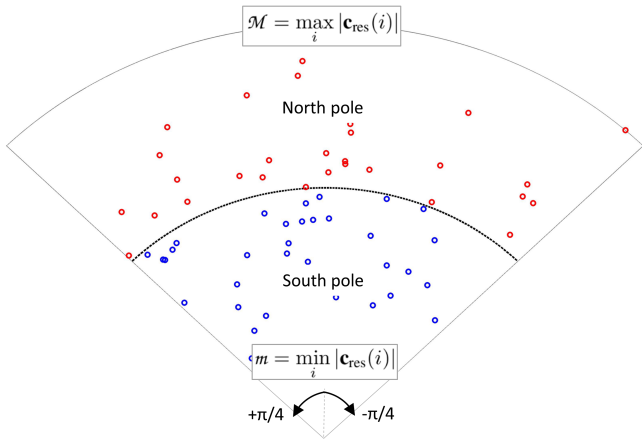
Fig. 3. Illustrative example of the geometric approach to find the parameter δ required for the residual update strategy in Algorithm 1 (case with 64 antenna elements).

the directions scanned simultaneously.

Algorithm 1 outlines the pseudo-code of our greedy, geometric strategy to approximate the fully-digital codebook $\mathbf{C}_{\text{bsl}}$ by a hybrid analog-digital architecture with 2-bit RF phase shifters. The algorithm takes as input parameter the baseline combiner to approximate, $\mathbf{C}_{\text{bsl}}$. Then, it initializes $\mathbf{C}_{\text{RF}}$ and the residual matrix $\mathbf{C}_{\text{res}}$. The algorithm proceeds by selecting from $\mathbf{C}_{\text{res}}$ the residual column $\mathbf{c}_{\text{res}}$ with maximum norm and appending its mapped version $\mathcal{S}(\mathbf{c}_{\text{res}}) \in \mathcal{C}_{\text{RF}}$ to the current RF combiner $\mathbf{C}_{\text{RF}}$ (lines 4-6). We denote $\mathcal{S}(\mathbf{v})$ an operator that maps the vector $\mathbf{v}$ into one close vector attainable with 2-bit RF phase shifters, i.e., a vector from the dictionary $\mathcal{C}_{\text{RF}}$. In other words, $\mathcal{S}(\mathbf{v})$ maps each component $\mathbf{v}(\ell)$ to the nearest value $e^{j\phi_\ell}$, being $\phi_\ell \in \left\{ -\frac{\pi}{2}, 0, \frac{\pi}{2}, \pi \right\}$.

Lines 7-14 refer to the residual update strategy which represent the core of the algorithm. The objective is to make $\mathbf{c}_{\text{res}} = \mathbf{c}_{\text{res}} - \delta \mathcal{S}(\mathbf{c}_{\text{res}})$ close to zero (not in norm) which equivalently translates into finding a value of $\delta \in \mathbb{C}$ such that:

$$\mathbf{c}_{\text{res}}(i) - \delta S(\mathbf{c}_{\text{res}})(i) \approx 0 \qquad \forall i \leq M_{\text{MS}} \qquad (6)$$

Mean square error minimization is not a convenient criterion for selecting δ because, at each step, the goal is not only to find a good projection for the selected $\mathbf{C}_{\text{RF}}$, but also a favorable residual for the future $\mathbf{C}_{\text{RF}}$ component approximations. For this reason, we geometrically envision the problem of finding δ as equivalent to that of finding a good center for the set of points $\frac{\mathbf{c}_{\text{res}}(i)}{\mathcal{S}(\mathbf{c}_{\text{res}})(i)}$ which are distributed inside a 90° circular sector in the complex plane as illustratively shown in Fig. 3. In fact, since $\mathcal{S}(\mathbf{c}_{\text{res}})$ maps the components of $\mathbf{c}_{\text{res}}$ to the closest points with 2-bit quantized phase, each point $\frac{\mathbf{c}_{\text{res}}(i)}{\mathcal{S}(\mathbf{c}_{\text{res}})(i)}$ has a complex argument between $-\pi/4$ and $\pi/4$ and modulus $|\mathbf{c}_{\text{res}}(i)|$. In order to find a good center for this set of points, we first find the maximum $\mathcal{M} = \max_i |\mathbf{c}_{\text{res}}(i)|$ and the minimum $m = \min_i |\mathbf{c}_{\text{res}}(i)|$. Then, we divide the 90° circular sector into two sub-sectors, namely the north pole which includes the points with modulus greater than or equal to $(\mathcal{M}+m)/2$ and the south

pole which includes the remaining points. Since, because of the shape of the circular sector, the points in the south pole have less variance compared to the points in the north pole, we focus on the latter, more representative points and calculate their mean value δ'. In line 8 of Algorithm 1, J is the set of indices relative to the elements of $\mathbf{c}_{\text{res}}$ falling within the north pole of Fig. 3, while the operator "/" in line 9 represents the element-wise division. If δ' falls within the north pole, we set δ to be on the "equator", i.e., $\delta = \frac{\mathcal{M}+m}{2} \frac{\delta'}{|\delta'|}$; otherwise, we set $\delta = \delta'$. The residual matrix is updated in lines 15-19.

The process continues until all $N_{\text{MS-RF}}$ beamforming vectors have been selected. Finally, the algorithm normalizes the digital baseband combining vector $\hat{\mathbf{C}}_{\text{BB}}$ to satisfy the constraint $\|\mathbf{C}_{\text{RF}}[\mathbf{C}_{\text{BB}}]_{:,i}\|_2^2 = 1$, for $i = 1, 2, ..., D$, and outputs it along with the constructed RF precoding matrix $\mathbf{C}_{\text{RF}}$.

Algorithm 1 can be used with only minor modifications to design hybrid analog-digital beam patterns at the BS side as well. In this case, since we are assuming that the BS transmits over one sector at a time, the required input parameter for the algorithm is the baseline precoding vector $\mathbf{p}_{\text{bsl}}$ to approximate, which is calculated according to the FSM-KW design outlined in [17]. In this case, the output provided by the algorithm is the RF precoding matrix $\mathbf{P}_{\text{RF}}$ and the baseband precoding vector $\mathbf{p}_{\text{BB}}$ given by:

$$\mathbf{p}_{\text{BB}} = \left(\mathbf{P}_{\text{RF}}^H \mathbf{P}_{\text{RF}} \right)^{-1} \mathbf{P}_{\text{RF}}^H \mathbf{p}_{\text{bsl}}$$
$$\mathbf{p}_{\text{BB}} = \frac{\mathbf{p}_{\text{BB}}}{\|\mathbf{P}_{\text{RF}}\mathbf{p}_{\text{BB}}\|_2} \qquad (7)$$

An implementation of the example proposed in Fig. 2 with ideal sectors is shown in Fig. 4, where beam patterns resulting from applying the proposed algorithm (solid blue/red line) are compared with the baseline fully-digital beamforming scheme based on FSM-KW (dashed black line). All the patterns are generated by a device having 64, $\lambda/2$-spaced isotropic antenna elements. As for the hybrid analog-digital design, an architecture consisting of 2-bit RF phase shifters and 10 RF chains is considered. As evident from the plots, the proposed algorithm is able to synthesize multi-beam patterns with limited overlap between adjacent beams and excellent flatness over the covered sectors. Furthermore, it is worth noting that, even with very low complexity hardware, the designed hybrid beam patterns are almost indistinguishable from the baseline fully-digital ones.

V. SIMULATION RESULTS

In this section, we present simulation results to evaluate the performance achieved by leveraging the proposed hybrid analog-digital beam patterns for adaptive beam training. Specifically, we split the problem into two phases as shown in Fig. 5. In the first phase, the BS and MS use Algorithm 1 to shape their beam patterns and apply the adaptive beam training protocol of §III to estimate the mmWave channel parameters, i.e., the most powerful AoD/AoA and the respective path gain. After the beam training, in a second phase, BS and MS leverage the geometric structure of the channel to construct the estimated channel matrix and build their hybrid data precoder
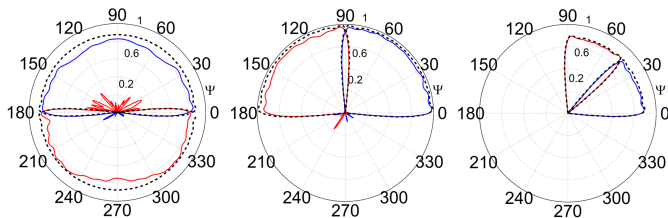
Fig. 4. Beam patterns for the first three stages of the beam training protocol. Comparison between the proposed hybrid analog-digital design (solid plot) and the baseline fully-digital design based on FSM-KW (dashed, black plot).
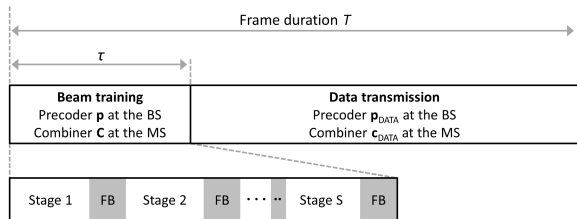

Fig. 5. Frame structure encompassing both beam training with feedback and data transmission.

$\mathbf{p}_{\text{DATA}}$ (at the BS) and data combiner $\mathbf{c}_{\text{DATA}}$ (at the MS) to approximate the dominant singular vectors of the estimated channel. Note that, compared to $\mathbf{C}$, which is the matrix used by the MS to combine multiple, simultaneous measurements during beam training, $\mathbf{c}_{\text{DATA}}$ is a vector since, for simplicity, we are considering data transmission through only one dominant path in the channel.

In a first set of simulations, we analyze the performance of the beam training protocol when varying the number of simultaneous directions D scanned by the MS. Concretely, in order to quantify the quality of the channel estimation achieved during the beam training phase, we consider the actual spectral efficiency (also referred to as rate in the sequel) experienced in the data transmission period $T - \tau$, which is given by the rate expression:

$$R = \log_2 \left| 1 + \text{SNR} \left| \mathbf{c}_{\text{DATA}}^H \mathbf{H} \mathbf{p}_{\text{DATA}} \right|^2 \right| \tag{8}$$

where SNR is the average signal-to-noise ration when omni-directional antennas are used at both the BS and MS.

For the simulations, we consider one BS with $M_{\text{BS}} = 64$ antennas and $N_{\text{RF-BS}} = 10$ RF chains, and one MS with $M_{\text{MS}} = 24$ and $N_{\text{RF-MS}} = 6$ RF chains, both featuring the hybrid analog-digital architecture of Fig. 1 and running the beam training algorithm described in §III. The distance between the BS and MS is set to 30m, and the path loss exponent is fixed to $n_{\text{ple}} = 3$. The antenna arrays are ULAs with $\lambda/2$-spaced isotropic radiators. We align with the simulation scenario in [16] and [17], which consider the channel model described in Eq. 2 with a number of paths $L = 3$ and the AoDs/AoAs taking continuous values uniformly distributed in $[0, 2\pi]$. The transmit power at the BS is set to 30dBm and the system is assumed to operate at 28-GHz carrier frequency
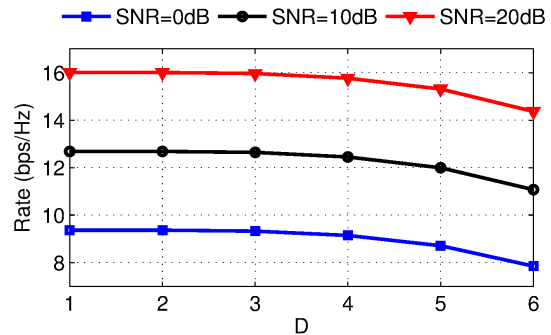

Fig. 6. Spectral efficiency when varying the number of simultaneously scanned directions D during beam training with $K = 6$. The figure compares the performance for different SNR values.

with 100-MHz bandwidth. All the numerical results provided in this section are obtained from Monte Carlo simulations with 5000 independent channel realizations for each BS/MS configuration.

The results in Fig. 6 indicate that, fixing the SNR, comparable spectral efficiencies are achieved for $D \leq 3$, while rate degradation is experienced for $D > 3$. The reason for this behavior is that, for a given number of RF chains, increasing D likewise increases the complexity of the beam patterns that are to be approximated. Hence, the quality of the beam shapes, and consequently of the channel estimation, strongly depends on the number of RF chains in respect of D. Exhaustive simulations, omitted for lack of space, reveal that, in general, keeping $D \leq N_{\text{RF-MS}}/2$ represents the best choice to not incur performance degradation.

In a second set of simulations, we analyze the impact of accelerating the beam training phase on the average data communication rate. To this end, differently from the previous set of simulations, we consider now the normalized spectral efficiency within a frame which is obtained by multiplying the rate R in Eq. 8 by the term $1 - \tau/T$. We consider the same simulation parameters of the previous analysis and the frame structure based on the work in [22]. Each frame of length $T = 10$ms is split in time into 100 slots of length $T_{\text{slot}} = 100\mu$s, a sufficiently small value to ensure channel coherence at mmWaves.

Figure 7 shows the normalized spectral efficiency achieved when the proposed multi-beam reception strategy is exploited at the MS. The performance is also compared with our prior work [17] and the reference paper [16], both adopting sequential reception at the MS during beam training. The beam training durations — τ and τ_{seq} respectively for our strategy and the sequential strategies — are calculated as described in §III. As evident from the plots, the ability of the proposed approach to speed up the beam training phase (or, equivalently, to reduce the training overhead) directly improves the normalized spectral efficiency since more time can be used for actual data transmission. More concretely, our approach provides a rate only 18% smaller than the ideal rate (i.e., assuming perfect channel knowledge) and, roughly,
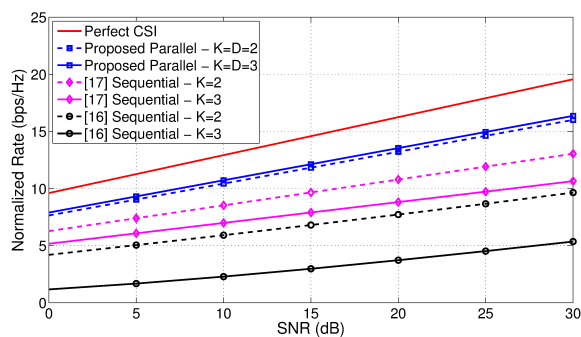
Fig. 7. Normalized spectral efficiency when varying the SNR: comparison with the literature for different values of D and K.

25% and 70% greater than [17] and [16] respectively. It is worth recalling that the proposed strategy relies on a hybrid analog-digital transceiver architecture with only 2-bit RF phase shifters in contrast to the 7-bit RF phase shifters considered in [16].

Finally, taken collectively, the presented results demonstrate how the proposed protocol is able to significantly accelerate the mmWave beam training process by means of parallel, multi-beam reception at the MS. Such an acceleration directly translates in a considerable increase of the data transmission rate compared with the literature.

VI. Conclusion

In this paper, we proposed and implemented an adaptive, low-overhead beam training protocol exploiting the simultaneous, multi-direction scanning capabilities of hybrid analog-digital transceivers operating at mmWave frequencies. To accomplish that, we derived a practical codebook design for hybrid architectures with a number of RF chains much lower than the number of antenna elements and only 2-bit RF phase shifters. Compared almost to the totality of approaches in the literature, which are based on the OMP algorithm, we relied on a novel, geometric strategy to approximate a fully-digital beamforming design with much lower computational complexity and higher accuracy. Simulation results showed that our hybrid codebooks are able to shape beam patterns almost indistinguishable from those attained by fully-digital beamforming, yet requiring lower complexity hardware compared with the literature. Moreover, the speed up of the beam training phase, in turn enabled by the multi-beam characteristics of our hybrid codebooks, provided a 25% to 70% increase in spectral efficiency compared to state-of-the-art strategies that adopt sequential, single-direction scanning during beam training.

ACKNOWLEDGMENTS

We thank Per Zetterberg for his very helpful comments about this work.

The research leading to these results received funding from the European Commission H2020 programme under grant agreement no 671650 (5G PPP mmMAGIC project). This article was also partially supported by the Madrid Regional Government through the TIGRE5-CM program (S2013/ICE-2919), the Ramon y Cajal grant from the Spanish Ministry of Economy and Competitiveness RYC-2012-10788, and the European Research Council grant ERC CoG 617721.

References

[1] T. S. Rappaport *et al.*, "Millimeter wave mobile communications for 5G cellular: It will work!" *IEEE Access*, vol. 1, pp. 335–349, May 2013.

[2] mmMAGIC. Millimetre-Wave Based Mobile Radio Access Network for Fifth Generation Integrated Communications, EU 5G-PPP H2020-ICT-2014-2 Project. [Online]. Available: http://5g-mmmagic.eu/

[3] A. Valdes-Garcia *et al.*, "A SiGe BiCMOS 16-element phased-array transmitter for 60Ghz communications," in *2010 IEEE Solid-State Circuits Conference (ISSCC)*, Feb. 2010.

[4] J. Wang *et al.*, "Beam codebook based beamforming protocol for multi-Gbps millimeter-wave WPAN systems," *IEEE Journal on Selected Areas in Communications*, vol. 27, no. 8, pp. 1390–1399, Oct. 2009.

[5] L. Chen, Y. Yang, X. Chen, and W. Wang, "Multi-stage beamforming codebook for 60GHz WPAN," in *2011 6th Int. ICST Conference on Communications and Networking in China (CHINACOM)*, Aug. 2011.

[6] S. Hur *et al.*, "Millimeter wave beamforming for wireless backhaul and access in small cell networks," *IEEE Transactions on Communications*, vol. 61, no. 10, pp. 4391–4403, Oct. 2013.

[7] Y. Tsang, A. Poon, and S. Addepalli, "Coding the beams: Improving beamforming training in mmwave communication system," in *2011 IEEE Global Telecommunications Conference (GLOBECOM)*, Houston, TX, USA, Dec. 2011.

[8] D. Pepe and D. Zito, "A novel phase shifter for 60 Ghz phased arrays," in *2015 Irish Signals and Systems Conf. (ISSC)*, Jun. 2015.

[9] T. Nitsche, G. Bielsa, I. Tejado, A. Loch, and J. Widmer, "Boon and bane of 60 GHz networks: Practical insights into beamforming, interference, and frame level operation," in *The 11th Int. Conference on emerging Networking EXperiments and Technologies (CoNEXT 2015)*, Dec. 2015.

[10] H. Shokri-Ghadikolaei, L. Gkatzikis, and C. Fischione, "Beam-searching and transmission scheduling in millimeter wave communications," in *2015 IEEE Int. Conference on Communications (ICC)*, June 2015.

[11] A. Loch, I. Tejado, and J. Widmer, "Potholes ahead: Impact of transient link blockage on beam steering in practical mm-Wave systems," in *European Wireless Conference 2016*, May 2016.

[12] C. N. Barati *et al.*, "Directional cell discovery in millimeter wave cellular networks," *IEEE Transactions on Wireless Communications*, vol. 14, no. 12, pp. 6664–6678, Dec. 2015.

[13] S. Payami, M. Shariat, M. Ghoraishi, and M. Dianati, "Effective RF codebook design and channel estimation for millimeter wave communication systems," in *2015 IEEE International Conference on Communication Workshop (ICCW)*, Jun. 2015.

[14] J. Song, J. Choi, and D. J. Love, "Codebook design for hybrid beamforming in millimeter wave systems," in *2015 IEEE International Conference on Communications (ICC)*, London, UK, Jun. 2015.

[15] O. E. Ayach, R. W. Heath, S. Abu-Surra, S. Rajagopal, and Z. Pi, "Low complexity precoding for large millimeter wave MIMO systems," in *2012 IEEE International Conference on Communications (ICC)*, Jun. 2012.

[16] A. Alkhateeb, O. E. Ayach, G. Leus, and R. W. Heath, "Channel estimation and hybrid precoding for millimeter wave cellular systems," *IEEE Journal of Selected Topics in Signal Processing*, vol. 8, no. 5, pp. 831–846, Oct. 2014.

[17] D. De Donno, J. Palacios, D. Giustiniano, and J. Widmer, "Hybrid analog-digital beam training for mmwave systems with low-resolution RF phase shifters," in *2016 IEEE ICC Workshop on 5G RAN Design*, May 2016.

[18] A. Sayeed, "Deconstructing multiantenna fading channels," *IEEE Transactions on Signal Processing*, vol. 50, no. 10, pp. 2563–2579, Oct. 2002.

[19] O. El Ayach, S. Rajagopal, S. Abu-Surra, Z. Pi, and R. Heath, "Spatially sparse precoding in millimeter wave mimo systems," *IEEE Transactions on Wireless Communications*, vol. 13, no. 3, pp. 1499–1513, Mar. 2014.

[20] A. Alkhateeb, O. E. Ayach, G. Leus, and R. W. Heath, "Single-sided adaptive estimation of multi-path millimeter wave channels," in *2014 IEEE 15th International Workshop on Signal Processing Advances in Wireless Communications (SPAWC)*, Jun. 2014.

[21] S. J. Orfinidas, "Electromagnetic waves and antennas," http://www.ece.rutgers.edu/~orfanidi/ewa/, (Visited on June 8th, 2016).

[22] F. Khan and Z. Pi, "mmWave mobile broadband (MMB): Unleashing the 3–300Ghz spectrum," in *34th IEEE Sarnoff Symposium*, May 2011.